Fluid Phase Equilibria 562 (2022) 113556

Contents lists available at ScienceDirect

Fluid Phase Equilibria

journal homepage: www.journals.elsevier.com/fluid-phase-equilibria

Selection of hydrotropes for enhancing the solubility of artemisinin in aqueous solutions

Isabela Sales [a,b], Dinis.O. Abranches [b], Tânia E. Sintra [b], Silvana Mattedi [a], Mara G. Freire [b], João A.P. Coutinho [b], Simão P. Pinho [c,*]

[a] Escola Politécnica, Universidade Federal da Bahia, Salvador, Bahia, 40210-630, Brazil
[b] CICECO – Aveiro Institute of Materials, Department of Chemistry, University of Aveiro, 3810-193 Aveiro, Portugal
[c] Mountain Research Center – CIMO, Polytechnic Institute of Bragança, 5301-855 Bragança, Portugal

ARTICLE INFO

Keywords:
Artemisinin
Ionic liquids
Salts
Aqueous solubility
Solvatochromic parameters
COSMO-RS

ABSTRACT

Artemisinin is an antimalarial substance very sparingly soluble in water. In the attempt to identify environmental-friendly and non-toxic aqueous-based solvents to extract it from *Artemisia annua L.,* the solubility of artemisinin in aqueous solutions of different hydrotropes was measured at 303.2 K, for hydrotrope concentrations up to 5 M. The ability of the studied hydrotropes for enhancing the artemisinin solubility increases in the following order: $Na[N(CN)_2]$ < Na[SCN] < [Chol][Van] < [Chol][Gal] < $[N_{4,4,4,4}]Cl$ < [Chol][Sal] < $[P_{4,4,4,4}]Cl$ < Na[Sal], with Na[Sal] allowing an increase in the solubility of 750 fold compared to pure water.

The COSMO-RS model and experimental Kamlet-Taft solvatochromic parameters were applied to connect the solubility enhancement with solvent properties. At low hydrotrope concentration, the solubility increases with the decreasing of the difference between the Apolar Factors of the hydrotrope and artemisinin, while for higher hydrotrope concentration, the hydrogen-bond acceptor character of the hydrotrope seems to have an impact on the solubility enhancement. Even if some mechanistic understanding is still to unfold, quantitatively the empirical correlations of solubility enhancement with the hydrotrope concentration and the solvatochromic parameters show very high accuracy. In particular, 93% of the change on the artemisinin solubility enhancement could be explained using the hydrotrope concentration and two combined solvatochromic parameters ($\alpha\beta$ and π^{*2}) as explaining variables.

1. Introduction

The poor water solubility of active pharmaceutical ingredients is a central concern in the field because it is often connected to poor bioavailability, especially via oral administration [1]. Artemisinin is one of the most potent and rapidly acting antimalarial drugs [2] but presents very low solubility in water [3–7]. Therefore, some approaches have been developed to enhance the solubility and dissolution of this poorly water-soluble drug, such as drug-polymer complexation using a hydrophilic polymer [4] and a spray drier with a modified multi-fluid nozzle [8,9]. However, studies involving hydrotropic compounds to increase the solubility of artemisinin in water are still rare. They should be explored as they can contribute to improve the artemisinin solubility but also to increase its bioavailability [10–13].

Hydrotropes are amphiphilic compounds whose molecular structure usually presents both hydrophilic and hydrophobic parts [14,15]. Its mechanism of action is not entirely understood, but recent studies [11,16] connected the hydrotrope aggregation around the solute to the apolarity of both components. This seems to constitute the driving force to solute-hydrotrope interactions in aqueous solution [11,16]. In addition to the traditional hydrotropes like sodium salts of short alkylbenzene sulfonates, short-chain alcohols, and some small organic molecules like urea [17,18], ionic liquids (IL) have been reported as a promising class of hydrotropes. IL are organic salts with low melting points that can be assembled from many different ions [19,20], which for the purpose of this study is very interesting as both cation and anion contribute to the solubility increase of hydrophobic compounds in water [10,21,22]. It has been shown that imidazolium-based IL are good hydrotropes [10,23,24]. However, recent work indicates that other classes such as cholinium-based IL can also be used to increase the solubility of hydrophobic drugs like ibuprofen and naproxen [25]. The results showed that cholinium salicylate increases the solubility of ibuprofen up to

* Corresponding author.
E-mail address: spinho@ipb.pt (S.P. Pinho).

https://doi.org/10.1016/j.fluid.2022.113556
Received 6 January 2022; Received in revised form 15 July 2022; Accepted 18 July 2022
Available online 20 July 2022

6000-fold, which reveals an exceptional hydrotropic ability of cholinium-based ionic liquids.

Due to the success of imidazolium-based IL as hydrotropes for phenolic acids and other bioactive compounds [10,21,22], in a former study [24], the anion effect on the solubility of artemisinin in water for IL containing the 1-butyl-3-methylimidazolium cation was investigated. The current work aims to apply the knowledge gained on the studies of hydrotropic solubilization of bioactive compounds in aqueous solutions to the solubility of artemisinin. In this study, cations with larger hydrophobic regions such as tetrabutylammonium and tetrabutylphosphonium are considered, altogether with some cholinium- based ILs and salts. The set of compounds studied was chosen to extend the knowledge on the impact of the ions nature on the solubility of artemisinin. In order to rationalize the hydrotrope characteristics that favor artemisinin solubility enhancement, the solvatochromic parameters of these hydrotropes were also determined. In fact, solvatochromic probe studies offer direct information on solvent properties, such as dipolarity/polarizability and hydrogen-bond donating/accepting capabilities [26–28], which in this work are combined with COSMO-RS to establish relations between the artemisinin solubility enhancement and the solvent characteristics.

2. Experimental section

2.1. Materials

The structure of all ions composing the IL and the salts as well as of artemisinin are depicted in Fig. 1, and the source and purity of the chemicals used are shown in Table 1. The IL were dried in a vacuum line (0.1 Pa and 353.15 K) for 48 h prior to their use (the water content of the IL is less than 1500 ppm). Ultrapure water was used, which was doubly distilled, passed through a reverse osmosis system and treated in Milli-Q plus 185 water purification equipment.

2.2. Synthesis of cholinium-based IL

Three cholinium-based IL were synthesized here, choline gallate ([Chol][Gal]), choline vanillate ([Chol][Van]) and choline salicylate ([Chol][Sal]). They were produced by the neutralization of the base (choline bicarbonate, 1 mol equivalents) with the appropriate acid (gallic, vanillic, and salicylic acids, 1.1 mol equivalents). Although the synthesis has already been reported in the literature [29,30], the synthetic route proposed here is simpler since we used choline bicarbonate (instead of choline hydroxide), allowing synthesis without the need of a nitrogen atmosphere.

More specifically, choline bicarbonate was added dropwise into an aqueous acid solution at 273 K. The mixture was stirred overnight at room temperature and protected from light, producing the cholinium-based IL, carbon dioxide, and water as a by-product. The water was then removed under reduced pressure. The unreacted acid was eliminated by washing with methanol for [Chol][Gal], ethyl acetate for [Chol][Sal], and acetone for [Chol][Van], and the solution was filtered to remove the IL (which is in the solid state). The only exception was for

Table 1
Properties of the chemicals used, supplier, CAS and minimum purity.

Compound	Supplier	CAS	Minimum Purity (wt%)
Tetrabutylphosphonium chloride $[P_{4,4,4,4}]Cl$	Sigma	2304-30-5	99
Tetrabutylammonium chloride $[N_{4,4,4,4}]Cl$	Sigma	1112-67-0	99
Sodium salicylate Na[Sal]	Sigma	54-21-7	99
Sodium thiocyanate Na[SCN]	Fluka	540-72-7	98
Sodium dicyanamide $Na[N(CN)_2]$	Sigma	1934-75-4	98
Choline bicarbonate	Sigma	78-73-9	80
Gallic acid	Merck	149-91-7	99
Salicylic acid	Acofarma	69-72-7	99
Vanillic acid	Acros Organics	121-34-6	97
Ethyl acetate	VWR Chemicals	141-78-6	99
Methanol	Fisher Scientific	67-56-1	HPLC grade
Acetonitrile	Fisher Scientific	75-05-8	99
Artemisinin	Kang Biothec	63968-64-9	99

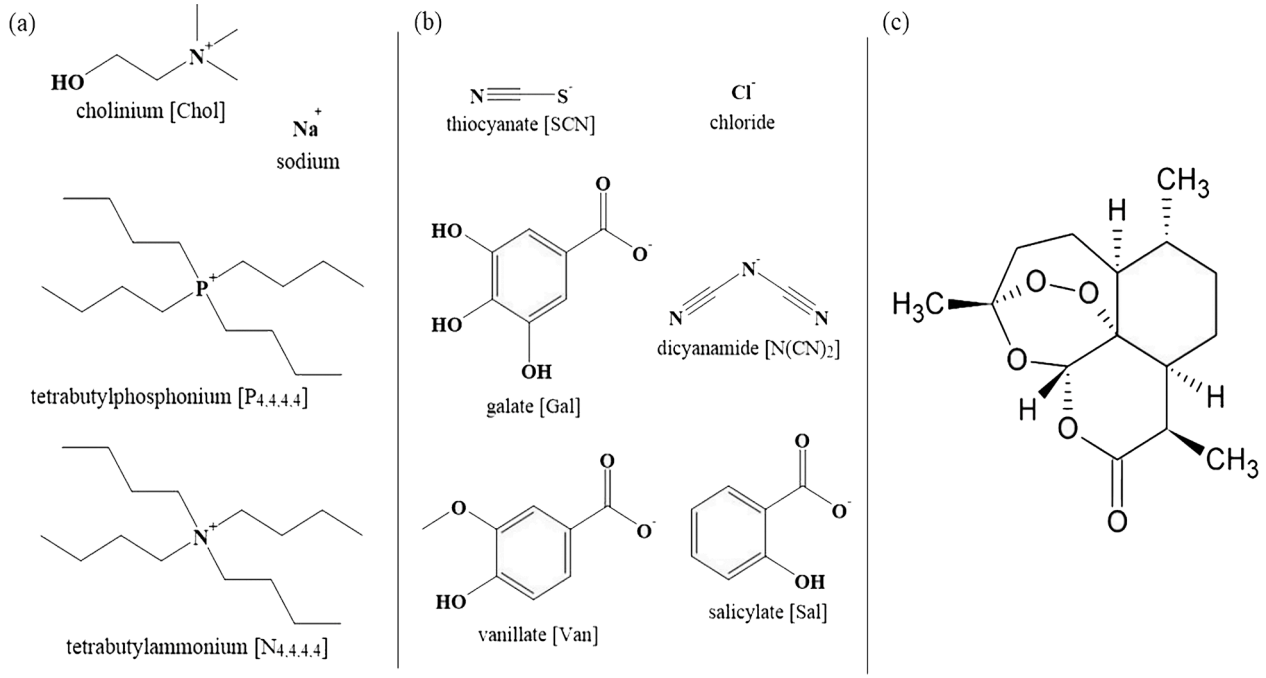

Fig. 1. Chemical structure of (a) cations and (b) anions of the studied hydrotropes and (c) artemisinin.

[Chol][Sal]. The remaining salicylic acid was accumulated as a viscous aqueous solution, being removed by liquid-liquid extraction. Finally, the residual solvent was removed under reduced pressure at 333 K, and the obtained compound was dried under a high vacuum for at least 48 h. The structure of all compounds synthesized was confirmed by ^{1}H and ^{13}C NMR (cf. Supporting Information, Figures S1 to S3), showing a high purity level of all synthesized substances.

2.3. Solubility of artemisinin

Aqueous solutions containing the ionic liquids were prepared gravimetrically, using a Mettler Toledo XS205 Dual Range balance (repeatability of 0.015 mg). Artemisinin in slight excess to the solubility limit was added to each eppendorf with the aqueous solutions and dispersed using a vortex. The system was left with constant stirring (750 rpm) and temperature of (303.2 ± 0.5) K for 72 h in the Eppendorf Thermomixer Comfort equipment, thus ensuring the saturation of artemisinin in the solution. After, the samples were centrifuged at 4500 rpm and (303.2 ± 0.5) K for 20 min using a Thermo Scientific Heraeus Megafuge 16R centrifuge. For each solvent, three independent saturation solutions were prepared.

Finally, the saturated solution was sampled, and a filtration step was performed using syringe filters (0.45 μm) acquired at Whatman, and after diluted in a mixture of acetonitrile and ultrapure water in a volumetric ratio of 60:40 when required.

2.4. Quantification of artemisinin

The amount of artemisinin was quantified by HPLC-DAD (Shimadzu, model PROMINENCE, with diode array detector SPD-M20A), using an analytical method previously developed by our group [21,24]. HPLC analyses were performed with an analytical C18 reversed-phase column (250 × 4.60 mm), kinetex 5 μm C18 100 A, from Phenomenex. The mobile phase consisted of 60% of acetonitrile and 40% of ultra-pure water (volume percentages). The separation was conducted in isocratic mode, at a flow rate of 1.0 mL·min^{-1} and using an injection volume of 10 μL. DAD was set at 210 nm. Each sample was analyzed at least in duplicate. The column oven and the autosampler were operated at a controlled temperature of 303.2 K. At these conditions, artemisinin displays a retention time of around 6 min. Calibration curves were prepared using pure (commercial) artemisinin, with concentrations ranging from 25 mg/L to 1000 mg/L.

2.5. Solvatochromic parameters

To obtain the parameter α (hydrogen-bond donating ability), the probe pyridine-N-oxide (PyO) was used, and following standard procedures, determined by ^{13}C nuclear magnetic resonance (NMR) spectra, using a Bruker Avance 300 equipment operating at 75 MHz, deuterium oxide (D_2O) as solvent and trimethylsilyl propanoic acid (TSP) as the internal reference. The ^{13}C NMR chemical shifts δ(Ci) in ppm of the carbon atoms in positions i = 2 and 4 of pyridine-N-oxide were determined, and α was calculated by [31–33]:

$$\alpha = -0.15 \cdot d_{24} + 2.32 \quad (1)$$

where $d_{24} = \delta_4 - \delta_2$.

The parameters β (hydrogen-bond acceptor ability) and π^* (solvent dipolarity/polarizability) were determined using the N,N-diethyl-4-nitroaniline (N,N), and 4-nitroaniline (4N) dyes, respectively. After vigorous stirring for the complete dissolution of the dyes, samples were scanned by UV-Vis spectrophotometer (BioTeck Synergy HT microplate reader). The longest wavelength absorption band of each probe was used in Eqs. (2) to (4) to determine the correspondent parameters.

$$\beta = \frac{0.76(\Delta\nu^{IL} - \Delta\nu^{cyclohexane})}{\Delta\nu^{DMSO} - \Delta\nu^{cyclohexane}} \quad (2)$$

$$\Delta\nu = \nu_{N,N} - \nu_{4N} \quad (3)$$

$$\pi^* = \frac{\left(\nu^{IL}_{N,N} - \nu^{cyclohexane}_{N,N}\right)}{\nu^{DMSO}_{N,N} - \nu^{cyclohexane}_{N,N}} \quad (4)$$

where, ν is the experimental wave number, and the superscripts IL, cyclohexane, and DMSO are correspondent to the values found in these solvents.

2.6. COSMO-RS

The σ-profile framework of COSMO-RS [34–36] was used in this work to compute molecular descriptors that quantify the polar and apolar surface areas of a molecule. To do so, the geometry of each individual ion was initially optimized using the BP-TZVP template of the quantum chemistry software package TURBOMOLE [37]. This template uses the def-TZVP basis set, the BP-86 DFT functional, and the COSMO solvation model with ideal screening (infinite permittivity). Given the relative simplicity of the molecular structure of the ions studied in this work, and the absence of multiple relevant conformers, only a single conformer was optimized for each ion. Then, the σ-profile of each individual ion was obtained using the BP_TZVP_21 parametrization of COSMOtherm [38]. Finally, the σ-profile of each ionic liquid was obtained by simply summing the σ-profiles of its individual ions, as illustrated in Supporting Information (Figure S4).

3. Results

3.1. Solubility of artemisinin

The solubility of artemisinin in pure water was determined in a previous work [24] and has a value of (61.83 ± 4.33) mg.L^{-1} at (303.2 ± 0.5) K. The impact of the hydrotrope concentration on the relative solubility of artemisinin is plotted in Fig. 2, while the complete data is compiled in Table S1 of the supporting information.

Among the studied compounds, some showed a remarkable hydrotropic effect for the antimalarial compound. The ability of the various IL and salts to act as hydrotropes for artemisinin increases in the following order: Na[N(CN)$_2$] < Na[SCN] < [Chol][Van] < [Chol][Gal] < [$N_{4,4,4,4}$]Cl < [Chol][Sal] < [$P_{4,4,4,4}$]Cl < Na[Sal].

The aqueous systems showing the highest hydrotrope effect ([Chol][Sal], [$P_{4,4,4,4}$]Cl, and Na[Sal]) show a significant change in the relative solubility at concentrations close to 1 mol/L. Some authors refer to this concentration as the minimum hydrotropic concentration (MHC), after which there is a significant increase in solubility [11,18,39], but without relating it to some change in the physicochemical properties or parameters of the solvent, making the concept questionable. On the other hand, the increase in the solubility of artemisinin in the aqueous solutions of others such as Na[N(CN)$_2$], Na[SCN] [Chol][Van], show a continuous increase in the solubility of artemisinin. These different behaviors corroborate the questioning of some authors regarding the existence of an MHC [14,40].

The solubility increase of artemisinin in some of the aqueous solutions does not follow a monotonic trend with the composition of IL. For example, aqueous solutions of [$P_{4,4,4,4}$]Cl and [Chol][Gal] show a decrease in solubility at concentrations between 1.0 and 2.0 mol.L^{-1}. This effect was previously observed for [C_4C_1im][N(CN)$_2$] and [C_4C_1im][TOS], and it can most probably be ascribed to hydrotrope self-interactions, decreasing its availability to interact with the solute [24]. Another possible explanation, as recently demonstrated for cirene-based systems [41], may be strong three-body interactions between water, solute, and hydrotrope, turning water a co-solvent for high hydrotrope concentration.

In order to evaluate the effect of the IL cation on the solubility of artemisinin, results are grouped in terms of the four different anions

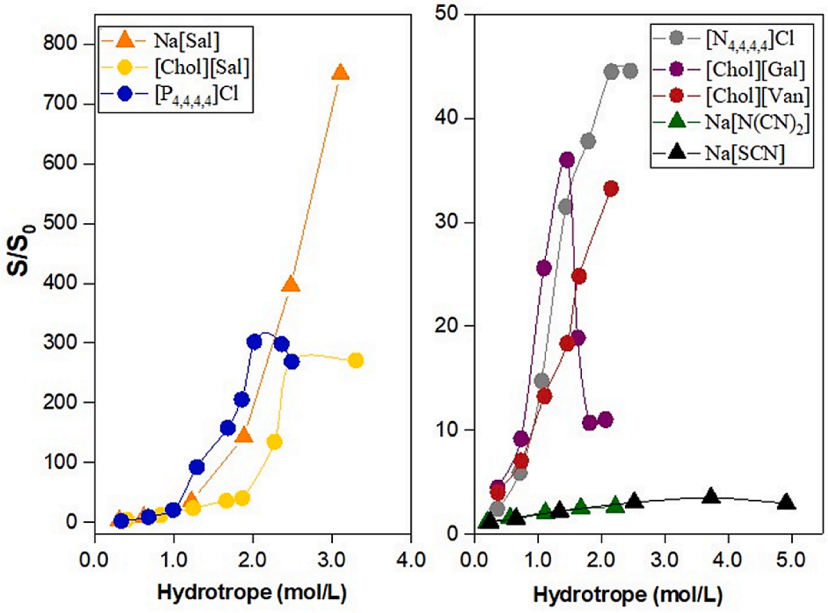

Fig. 2. Impact of the hydrotropes on the relative solubility of artemisinin at 303.2 K in aqueous solution. S and S_0 represent the solubility of artemisinin in the aqueous solution of the hydrotrope, and in water, respectively. The lines are just guides to the eyes.

studied. The series of chloride-based IL are shown in Fig. 3(a). Among the cations investigated in that series, $[P_{4,4,4,4}]^+$ clearly showed the most significant increase in the solubility of the drug studied in this work, followed by $[N_{4,4,4,4}]^+$ and $[C_4C_1im]^+$. Sintra et al. [21] reported a similar behavior of the hydrotropic effect of chloride-based IL on the solubility of ibuprofen.

As previously discussed [24], IL containing $[SCN]^-$ and $[N(CN)_2]^-$ are those that most increased artemisinin solubility in water. However, it is possible to see in Fig. 3b, c that the same behavior was not observed when these anions were combined with Na^+ instead of $[C_4C_1im]^+$. Unlike the IL, the two salts showed low to no hydrotropic effect on the solubility of artemisinin. This can be explained by the fact that the imidazolium cation has a large non-polar region, which has been shown to favor artemisinin solubilization, while Na^+ is mainly a point charge with no possibility to engage in dispersive interactions. In fact, it has been shown that the best-performing ionic hydrotropes are those that possess an ion with a large apolar volume and an amphiphilic counterion [22]. This explains why $[SCN]^-$ and $[N(CN)_2]^-$ salts show a good performance only when combined with the imidazolium cation. On the other hand, an impressive exception to this behavior is the effect of Na[Sal] (Fig. 3d). Aqueous solutions of this salt led to an almost 750-fold increase in the solubility of artemisinin, being unexpectedly the best among all the studied compounds. To confirm these results the solubility of artemisinin in aqueous Na[Sal] solutions was repeatedly measured in three independent periods by different researchers showing very high consistency.

In order to study the influence of the anion in the solubility of artemisinin, two groups were constituted; one formed by three IL based on the $[Chol]^+$ cation, and the other composed of three salts based on Na^+ (Fig. 4).

[Chol][Sal] is the IL that showed the greatest hydrotropic effect among IL with $[Chol]^+$ as a cation (Fig. 4a). In this case, increasing the substituents in the aromatic ring of the anion causes the IL to become more polar, causing a negative impact on the change of the solubility of artemisinin with the IL concentration. Among the salts (Fig. 4b), it is observed that small, linear cyanide anions have no significant hydrotropic effect when combined with Na^+, but were the best when combined with $[C_4C_1im]^+$, which demonstrates the impact of the interplay between the cation and the anion, as $[C_4C_1im]^+$ combined with chloride causes a much smaller effect on the artemisinin solubility. On the other hand, the salicylate anion has an aromatic ring in its structure, which is bulkier than the others (Fig. 4b), presenting a larger apolar volume (Fig. 4a) which favored, in both comparisons, the artemisinin solubility in the aqueous solution containing the salicylate anion.

COSMO-RS was applied to search for some insight on the hydrotropy behaviour in the studied systems. By analogy with the approach proposed by Abranches et al. [16], the sigma-profiles (Figures S4 to S6) were used to estimate the Apolar (AF) and the polar Donnor (DF) and Acceptor Factors (AcF), that allowed a quantification of the surface area of the different regions of the molecules. In the apolar region, the following equation was applied:

$$AF = \int_{-0.0082}^{0.0082} p(\sigma)(0.0082 - |\sigma|)d\sigma \quad (5)$$

While in the polar regions:

$$DF \text{ or } AcF = \int_{0.0082}^{|\sigma|} p(\sigma)(|\sigma| - 0.0082)d\sigma \quad (6)$$

The integrals were determined using the composite trapezoidal rule, and the results compiled in Table 2.

As shown in Fig. 5a, the results confirm the better hydrotropic ability of $[C_4C_1im][TOS]$ at concentrations up to 1.0 mol/L. Of all the systems studied, this compound has the more similar Apolar Factor to that of artemisinin (Table 2). On the other hand, the salts Na[SCN] and $Na[N(CN)_2]$ presenting an Apolar Factor very different from that of the artemisinin, are the compounds that showed a more negligible hydrotropic effect in this region. In fact, in this range of concentrations, it is generally observed that the hydrotropic effect is well correlated with the similarity between the Apolar Factor of the solute and the hydrotrope. Studying the hydrotropic effect on the solubility of gallic or syringic acid, Abranches et al. [16] showed that the number of hydrotrope molecules aggregating around the solute reaches a maximum when the Apolar Factor of the solute and the hydrotrope are equal, in good agreement with the results presented here.

In the range of higher hydrotrope concentration (Fig. 5b, c), it is possible to observe that the hydrogen-bond acceptor character begins to exert an impact on the solubility. In fact, the hydrotropes that cause the

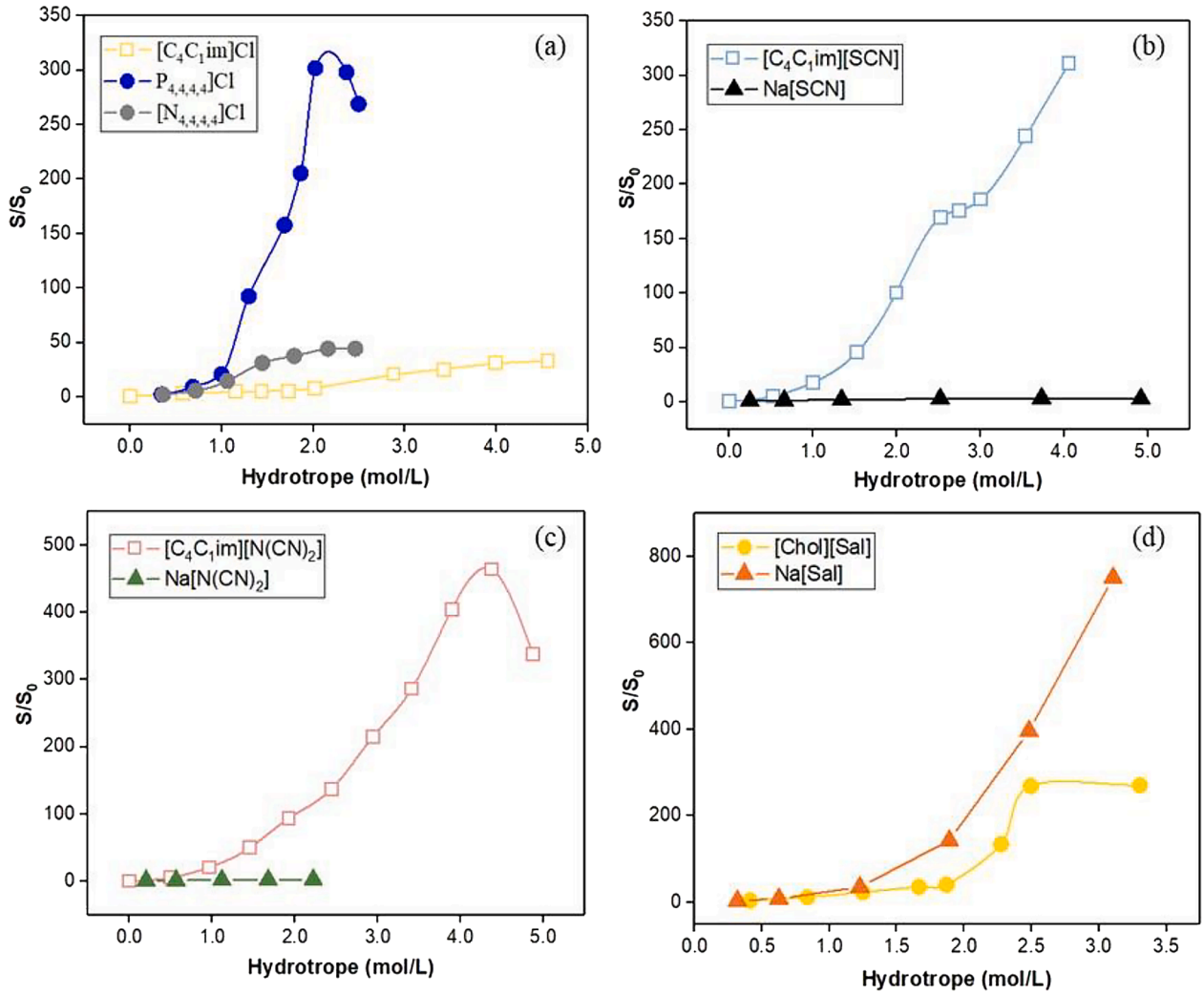

Fig. 3. Analyzing the cation effect on artemisinin solubility in aqueous solutions at 303.2 K. Hydrotropes are based on the anions (a) Cl^- (b) $[SCN]^-$ (c) $[N(CN)_2]^-$ and (d) $[Sal]^-$. Values for imidazolium-based IL were retrieved from [24]. The lines are guides to the eyes.

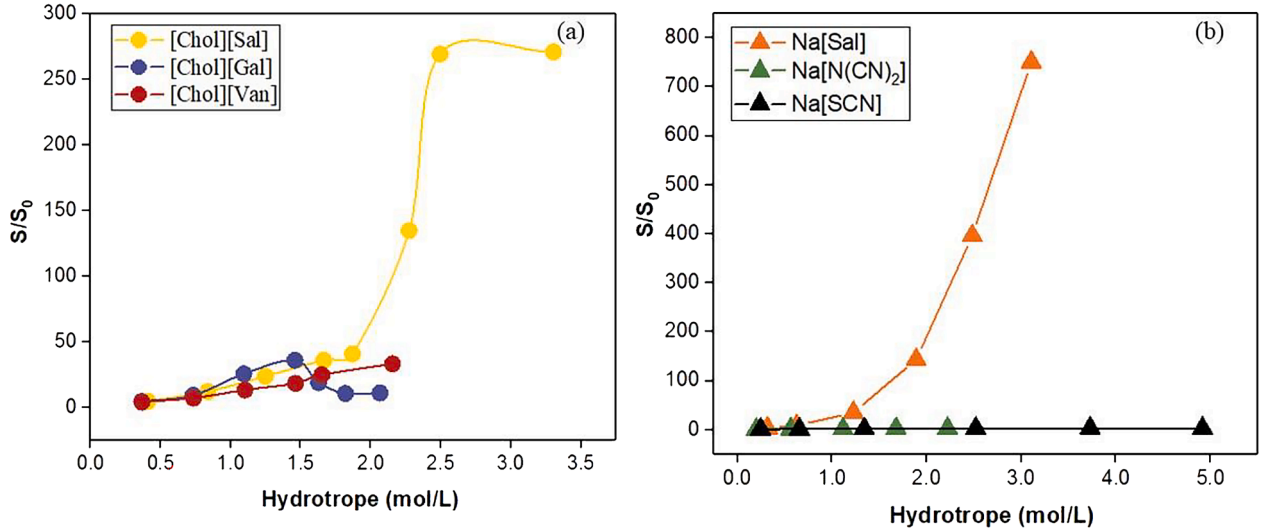

Fig. 4. Effect of anion on artemisinin solubility in aqueous solutions at 303.2 K. Hydrotropes are based on the cations (a) $[Chol]^+$ and (b) Na^+. The lines are guides to the eyes.

Table 2
Characteristic Factors (10000 e/Å^2) of the different regions; Donor, Acceptor, and Apolar, according to Eqs. (5) and (6).

	Donor	Apolar	Acceptor
Artemisinin	0.1	10.3	1.5
Water	1.0	0.4	0.7
$[C_4C_1im]Cl$	1.2	6.6	5.7
$[C_4C_1im][SCN]$	1.2	7.0	3.3
$[C_4C_1im][N(CN)_2]$	1.2	8.5	3.6
$[C_4C_1im][TOS]$	1.7	12.1	4.9
$[N_{4,4,4,4}]Cl$	0.4	15.9	5.7
$[P_{4,4,4,4}]Cl$	0.4	16.3	5.7
[Chol][Sal]	1.8	5.7	4.4
Na[Sal]	6.7	3.9	3.9
Na[SCN]	6.7	0.4	3.3
$Na[N(CN)_2]$	6.7	1.9	3.6

most significant increase in solubility ($[C_4C_1im][SCN]$, $[C_4C_1im][N(CN)_2]$ and Na[Sal]) have a moderate Acceptor Factor and, by increasing this value the hydrotropic effect is only maintained by simultaneously increasing the Apolar Factor. It can be seen that by fixing the anion, in all cases the solubility increases with the increase of the Apolar Factor. This situation also occurs by fixing the cation (sodium or $C_4C_1mim^+$), again demonstrating the importance of the Apolar Factor. The observation that Na[Sal] has the greatest increase in solubility is not, however, evident when compared to the effect of choline salicylate. Both have about the same Acceptor Factor, but in spite of its lower Apolar Factor, Na[Sal] induces a more considerable increase in the solubility of artemisinin. The sodium salts with dicyanamide and thiocyanate are the worst hydrotropes while Na[Sal] seems to be the best.

3.2. Solvatochromic parameters

In order to contribute to the understanding of the artemisinin solubility increase and the dominating solvent-solute interactions, the Kamlet-Taft parameters, α (hydrogen-bond donor, acidity), β (hydrogen-bond acceptor, basicity) and dipolarity/polarizability (were also determined. The effect of the IL concentration on the parameters is represented in Fig. 6 (the numerical values are compiled in Table S2). The methodology requires a colorless solution, however aqueous solution of [Chol][Gal] and [Chol][Van] are colored even at low concentrations thus the parameters for these ILs could not be determined.

Fig. 6 indicates that increasing the hydrotrope concentration, a decrease in the values of α is observed [42], with the exception of [Chol][Sal] solutions. The π^* parameter is the most affected by the presence of

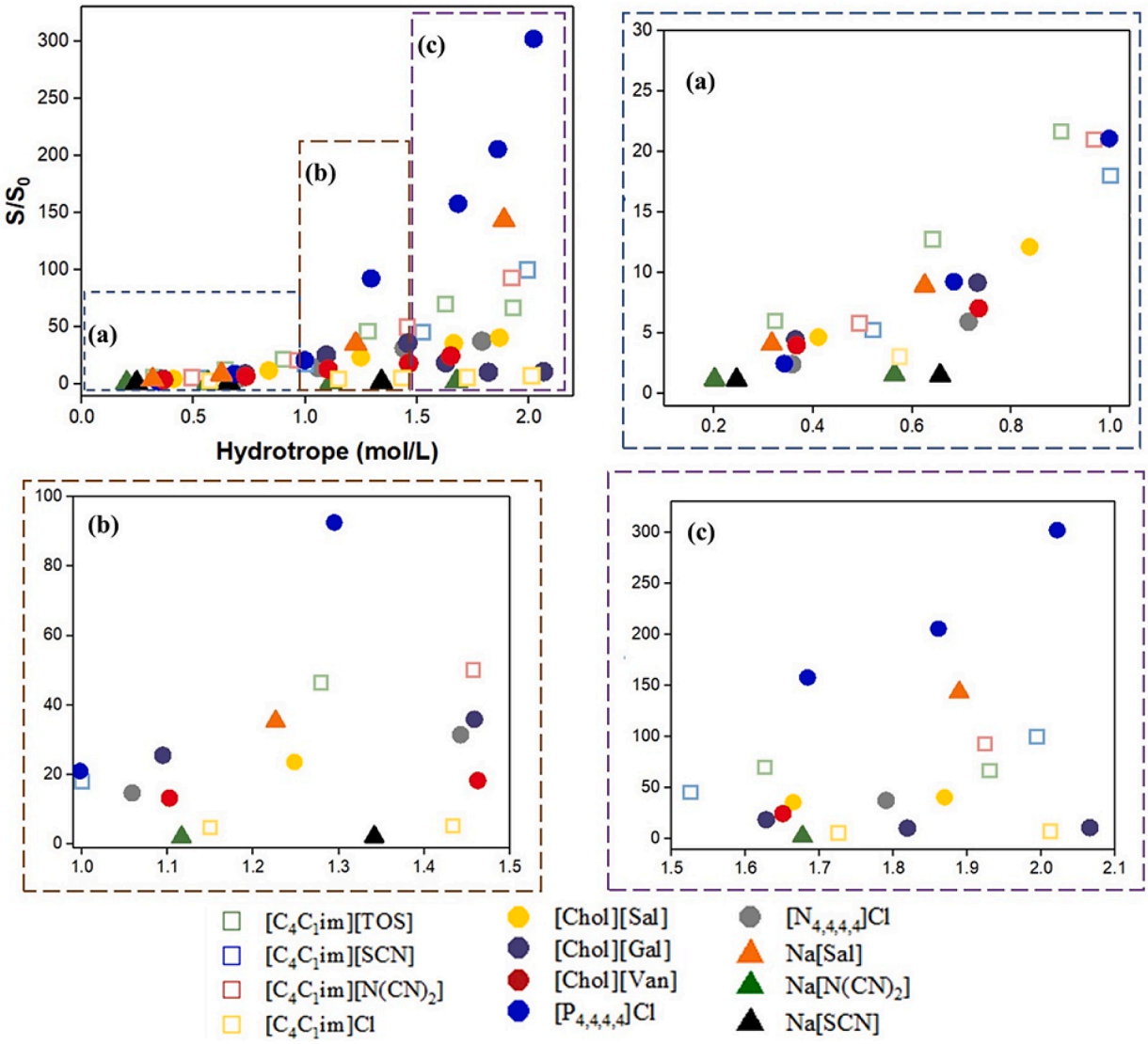

Fig. 5. Relative solubility of artemisinin at 303.2 K in low hydrotrope concentration for aqueous solutions of hydrotropes. Values for imidazolium-based IL were retrieved from [24].

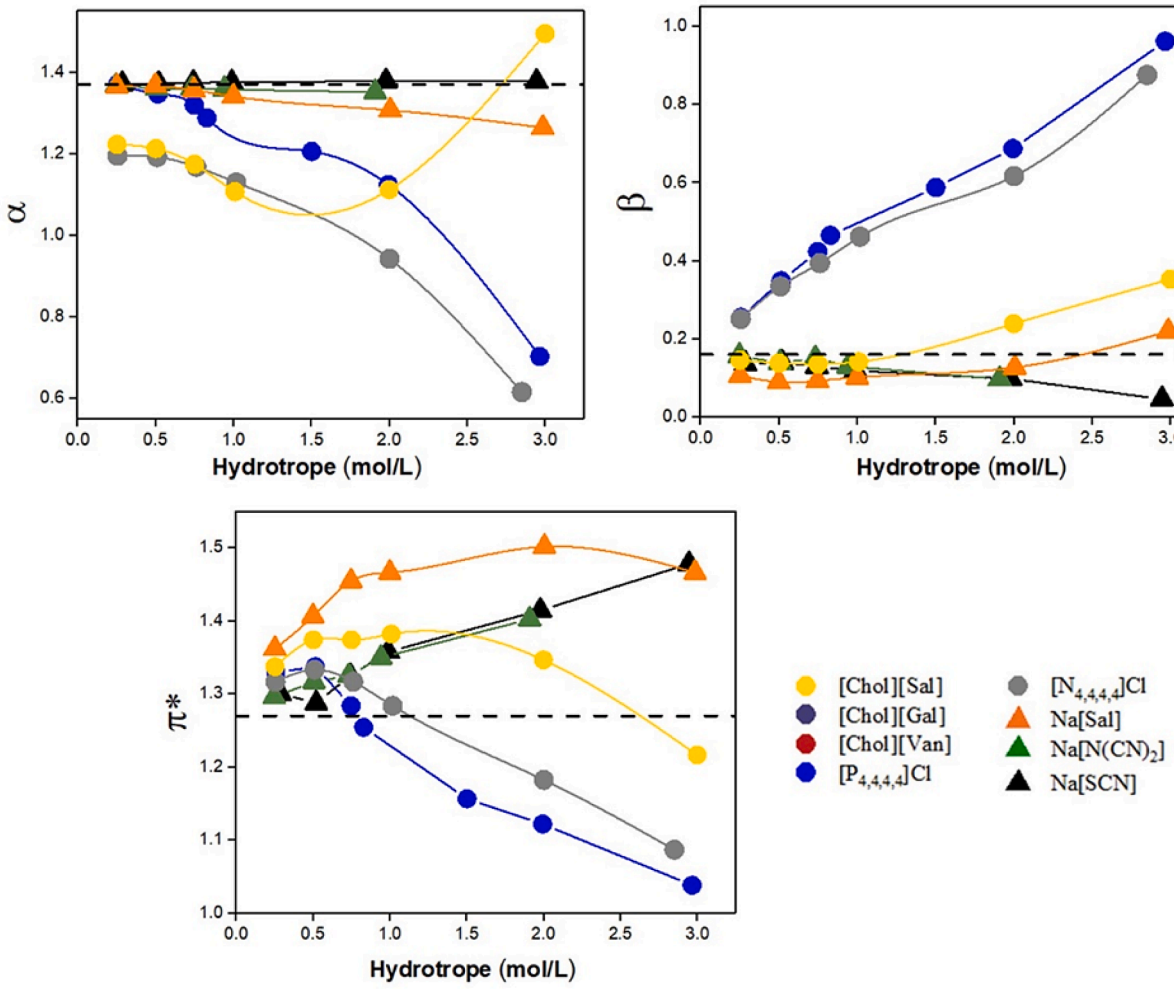

Fig. 6. Parameters α, β and π^* for aqueous solutions of hydrotropes. The dashed lines are the solvatochromic parameters for pure water [24]. The lines are guides to the eyes.

the hydrotrope and is higher than those of most molecular solvents [27]. Coulomb interactions, as well as dipole and polarizability effects, can justify this behavior [43,44]. As already reported [42], solutions with IL present a decrease of π^* with the concentration while the salts show the opposite behavior, presenting higher values than pure water. Concerning the hydrogen-acceptor (β) parameter, solutions of [Chol][Sal], [$P_{4,4,4,4}$]Cl, or [$N_{4,4,4,4}$]Cl show a similar behavior, increasing with the hydrotrope concentration, and is generally higher than that of pure water. Excepting sodium salicylate solutions, the other sodium salts show α and β parameters very close to pure water.

Some authors [43,45,46] point out that the strength of the hydrogen bond acceptor (β) of an IL is dominated by its anion, while the hydrogen bond donor capacity (α) is essentially controlled by the cation and depends only slightly on the IL anion. Based on this premise, and for better discussion on the behavior of the studied systems, the results of the parameters were grouped considering the different ions. Fig. 7 shows the experimental values for parameter α, for a common anion.

It is easily perceived that, in general, aqueous IL solutions behave very differently from salt solutions. Small cations, such as Na^+, have better donor characteristics when compared to cations such as $[C_4C_1im]^+$. Kurnia et al. [41] reported that IL bearing the imidazolium cation have higher α values than IL based on tetralkylammonium, among others. The high acidity of the imidazolium-based IL is mainly a result of the acidic hydrogen bonded to the carbon between the two nitrogen atoms in the ring. This would explain the results found in Fig. 7a, where the IL with aromatic ring ([C_4C_1im]Cl) has higher acidity than the non-aromatic ILs. The results found for α, are consistent with those presented above for the characteristic Factors (in Table 2), where it can be seen that the donor regions found in the sigma profiles are larger for salts than for imidazolium. In addition, when comparing the $[C_4C_1im]^+$ with $[P_{4,4,4,4}]^+$ and $[N_{4,4,4,4}]^+$, the behavior is also in accordance with that predicted by COSMO-RS, where the imidazolium has a greater hydrogen bond donating capacity than the other chlorinated IL studied here. In a previous work [24], it was shown that the value of α is also influenced by the anion, confirmed here for salt/IL solutions, even if in smaller magnitude (Fig. 8a). An interesting aspect is that the basicity of the aqueous solutions containing salts with -CN group (Fig. 8b) does not change with their number, in the same way as in ionic liquids aqueous solutions, while the trend in the basicity of Na[Sal] aqueous solutions is totally symmetrical to the acidity change with the salt concentration.

Among the sodium salts, there is a more evident influence of concentration on the acidity of aqueous solutions, mainly by Na[Sal]. As the donor region is numerically equal (Table 2) among these hydrotropes, the larger non-polar region of salicylate, when compared to the others, is the major contributor for this difference. Combined solvatochromic and COSMO-RS results suggest that the apolar region is the responsible to the reduction the acidity (α) of the Na[Sal] aqueous solutions. Furthermore, the β values are consistent with the sigma profiles generated by the COSMO-RS (Table 2), where $[Sal]^-$ has an acceptor region greater than $[N(CN)_2]^-$; followed by $[SCN]^-$, but surely a more complex interplay between all these regions contribute to the final outcomes.

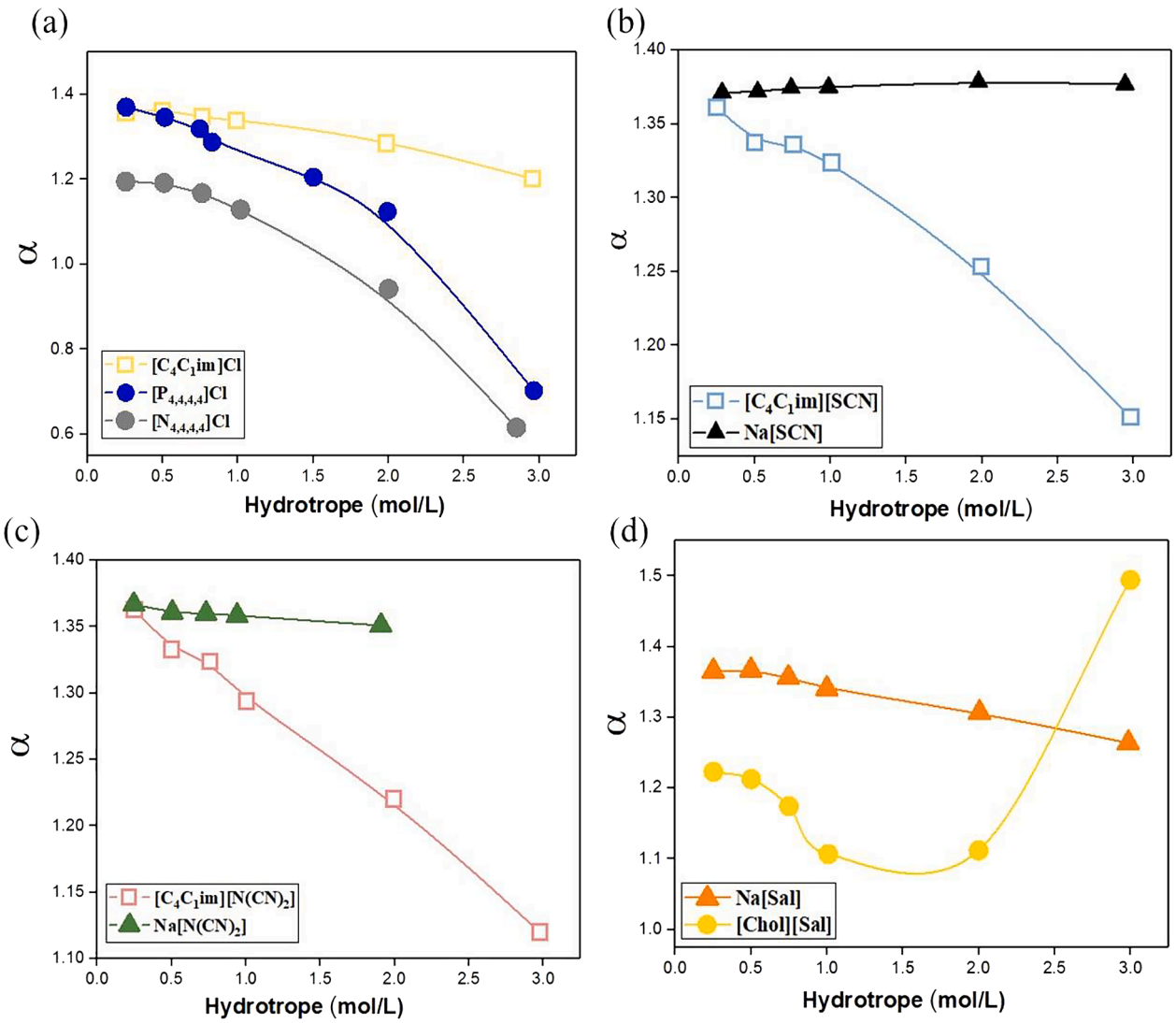

Fig. 7. Hydrogen-bond donor parameter for hydrotropes aqueous solutions based on: (a) Cl^-; (b) $[SCN]^-$; (c) $[N(CN)_2]^-$ and (d) $[Sal]^-$. The lines are guides to the eyes. Values for imidazolium-based IL were retrieved from [24].

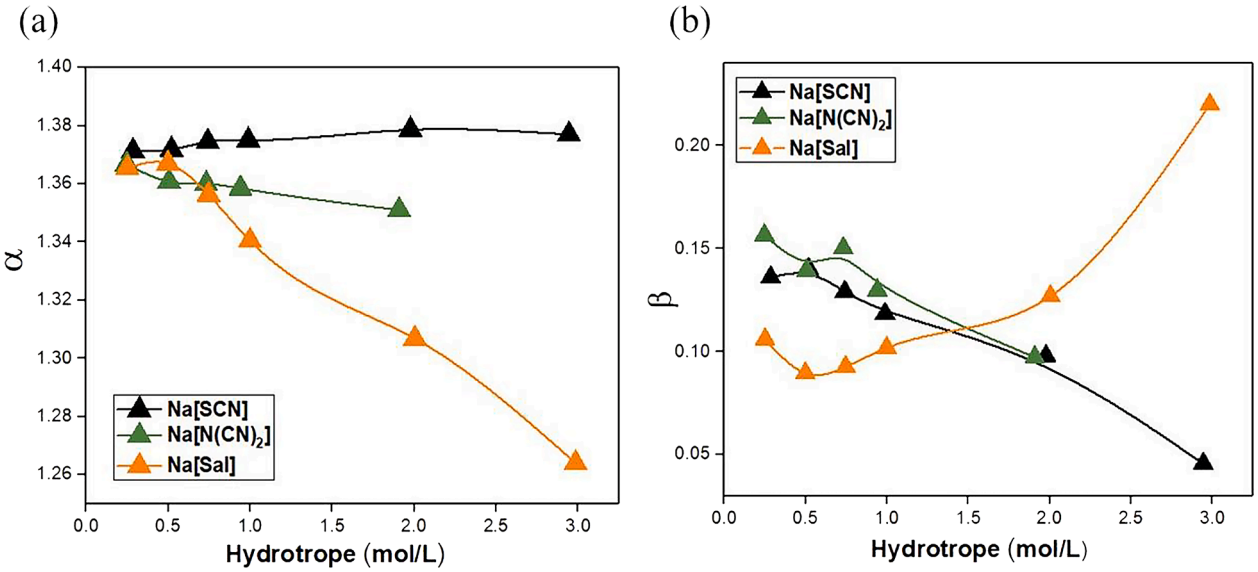

Fig. 8. Influence of anion on the hydrogen-bond (a) donor and (b) acceptor parameter for hydrotropes aqueous salt solutions. The lines are guides to the eyes.

An influence of the cation on the β parameter was also observed (Figure S7 of the supporting information). The results show quite good consistency as the results for β generally follow the reverse trend observed for α. The behavior of $[P_{4,4,4,4}]Cl$ and $[N_{4,4,4,4}]Cl$ solutions with increasing concentration varies similarly, in agreement with the large similarity between the cations. On the other hand, COSMO-RS acceptor region of [Sal]-based hydrotropes (Table 2) is larger for choline than for sodium, a behavior also observed in the β values, but not matching those for $[SCN]^-$ or $[N(CN)_2]^-$ based hydrotropes. Naturally, it should be emphasized that while COSMO-RS reflects the pure characteristics of the hydrotrope, the solvatochromic parameters characterize aqueous solutions of those compounds. Therefore, even if these associations are useful, the degree of dissociation of the hydrotropes into ions, ion-pairing (cation-anion interactions), interaction with water, play important roles, making difficult a straightforward approach connecting COSMO-RS to solvatochromic parameters.

Finally, the association between the non-polar region (from sigma profiles) of each hydrotrope and the π^* parameters was tested (Fig. 9 and Table 2). The results show that, in almost all systems evaluated, the increase in the non-polar region leads to a decrease in dipolarizability/polarizability. The exceptions are the sodium salts (Fig. 9e), showing that there is no clear parallel between the π^* values and the Apolar Factors reported in Table 2.

So far, a qualitative approach has been explored to explain the aqueous solubility enhancement of artemisinin in terms of the Kamlet-Taft parameters measured in this work. However, given that these parameters provide a holistic representation of the polarity (or lack thereof) of the hydrotrope aqueous solutions, a quantitative correlation may exist between them and the solubility of artemisinin. To test this hypothesis, linear/quadratic regressions were built between the natural logarithm of the aqueous solubility enhancement of artemisinin and the concentration of hydrotrope, the Kamlet-Taft parameters of the hydrotrope aqueous solution, and their combinations. These regressions can be written in a general manner as:

$$\ln(S/S_0) = f\left(C_H, \alpha, \beta, \pi^*, \alpha^2, \alpha\beta, \alpha\pi^*, \beta^2, \beta\pi^*, \pi^{*2}\right) \quad (7)$$

where C_H is the hydrotrope concentration (mol/kg), S/S_0 is the aqueous solubility enhancement of artemisinin in a hydrotrope solution of concentration C_H, and $\alpha, \beta, \pi^*, \alpha^2, \alpha\beta, \alpha\pi^*, \beta^2, \beta\pi^*$, and π^{*2} are the Kamlet-Taft parameters (and their combinations) of the hydrotrope aqueous solution at the same concentration.

All possible regressions based on Eq. 7 were tested (1024 combinations, using one to ten fitting variables), and the coefficient of determinations obtained are depicted in Fig. 10a). The performance of the linear correlation between $\ln(S/S_0)$ and C_H, π^*, and π^{*2} is depicted in Fig. 10b).

Fig. 10a reveals that a single variable (C_H) is enough to obtain a correlation with a coefficient of determination of 0.73. In fact, given the set of all possible 1-variable correlations, C_H clearly outperforms all other, which are the Kamlet-Taft parameters and their combinations. This is not surprising because the entire solubility curves obtained for each hydrotrope are being used (in the concentration range where Kamlet-Taft parameters were experimentally measured). In other words, for the same hydrotrope, $\ln(S/S_0)$ depends only on C_H. Fig. 10a also shows no significant increase of R^2 with the total number of variables of the correlation. In fact, with three variables (the best-performing combination being C_H, π^*, and π^{*2}), an R^2 of 0.80 is attained, while using all 10 variables, this value increases only to 0.84. Thus, the regression between $\ln(S/S_0)$ and C_H, π^*, and π^{*2}, which is depicted in Fig. 10b, is a good compromise between model performance and complexity.

The performance of the regression between $\ln(S/S_0)$ and C_H, π^*, and π^{*2}, depicted in Fig. 10b is quite good, in particular considering that only three variables are being used to correlate 72 independent data points. The fact that π^* and π^{*2} (together with C_H) appear as the most relevant variables to describe the change on $\ln(S/S_0)$ is in line with the current understanding of the mechanism of hydrotropy, where the apolar volume of the hydrotrope plays a central role in the solubility enhancement of the solute, as explored above [16]. This correlation is described by:

$$\ln(S/S_0) = 1.434 \cdot C_H - 106.8 \cdot \pi^* + 40.62 \cdot \pi^{*2} + 70.79 \quad (8)$$

It is noteworthy that the solubility data of $[C_4C_1im]Cl$ appears to be an outlier in the regression depicted in Fig. 10b. The cause of this is not yet clear. Nevertheless, the above procedure was repeated excluding the solubility data of $[C_4C_1im]Cl$ from the overall solubility dataset. Those results are depicted in Fig. 11a. The performance of the correlation between $\ln(S/S_0)$ and C_H, $\alpha\beta$, and π^{*2} is depicted in Fig. 11b.

Again, Fig. 11a shows that only one variable (C_H) is needed to accurately describe $\ln(S/S_0)$ when the solubility data for $[C_4C_1im]Cl$ is excluded, with an R^2 of 0.89. However, the coefficients of determination of the regressions reported in Fig. 11a are quite superior to those reported in Fig. 10a. This phenomenon does not seem to be just the result of decreasing the total number of data points (62 data points without $[C_4C_1im]Cl$), pointing, instead, to an unexpected abnormal behavior of $[C_4C_1im]Cl$.

In line with the results depicted in Fig. 10a, Fig. 11a shows that three fitting variables are a good compromise between model performance and complexity, with the best-performing 3-variables correlation achieving an R^2 of 0.93, while the full 10-variables correlation attains an R^2 of 0.97. However, contrary to the previous results, the omission of $[C_4C_1im]Cl$ from the dataset leads to C_H, $\alpha\beta$, and π^{*2} as the fitting variables of the best-performing 3-variables correlation, which is depicted in Fig. 11b. Note that the difference between the best 3-parameter variables, with and without $[C_4C_1im]Cl$, is π^* or $\alpha\beta$, respectively. This correlation is described by Eq. 9:

$$\ln(S/S_0) = 1.798 \cdot C_H + 3.426 \cdot \alpha\beta + 2.509 \cdot \pi^{*2} - 4.710 \quad (9)$$

The significance of $\alpha\beta$ in the correlation described above must be related to ion-ion interactions. Since $\alpha\beta$ is a descriptor of the cross-interaction between positive and negative polarities of the hydrotropic aqueous solutions, and because the major contributors to those polarities are most likely the ions of the ionic liquids and salts, $\alpha\beta$ represents the interaction strength of the hydrotrope ions. As shown in a previous work [22], the performance of ionic hydrotropes depends on the ability of their ions to simultaneously aggregate around the solute, to minimize the local charge of the cluster. It can be speculated that larger $\alpha\beta$ values lead to stronger cation-anion interactions and thus easier aggregation of cations and anions around the solute.

4. Conclusions

The present work focuses on studying IL and salts as potential hydrotropes for artemisinin. It is shown the excellent ability of Chol][Sal], $[P_{4,4,4,4}]Cl$, and Na[Sal] to increase artemisinin solubility in water, where the latter presents a maximum solubility increase of 750 fold compared to pure water. Furthermore, it is observed the dominant role of the apolar region on the rise of the solubility at low hydrotrope concentrations, which is very well correlated to the similitude of the Apolar Factor of artemisinin, with that of the hydrotrope, as calculated by COSMO-RS. For higher hydrotrope concentrations the hydrogen-bond acceptor character starts to exert an impact on the solubility. The best hydrotropes present a moderate acceptor character (COSMO-RS) and, increasing this value, the favorable hydrotropic effect is only maintained by simultaneously increasing the Apolar Factor.

The solvatochromic Kamlet-Taft parameters that describe the hydrogen-bond donor and acceptor character of the studied aqueous solutions, as well as their polarizability, were measured. In general, the results support the idea that both anion and cation synergistically influence α and β parameters. In contrast, the π^* parameter can be associated with the non-polar region of the hydrotropes. In general, the larger the non-polar region, the smaller the value of this parameter in

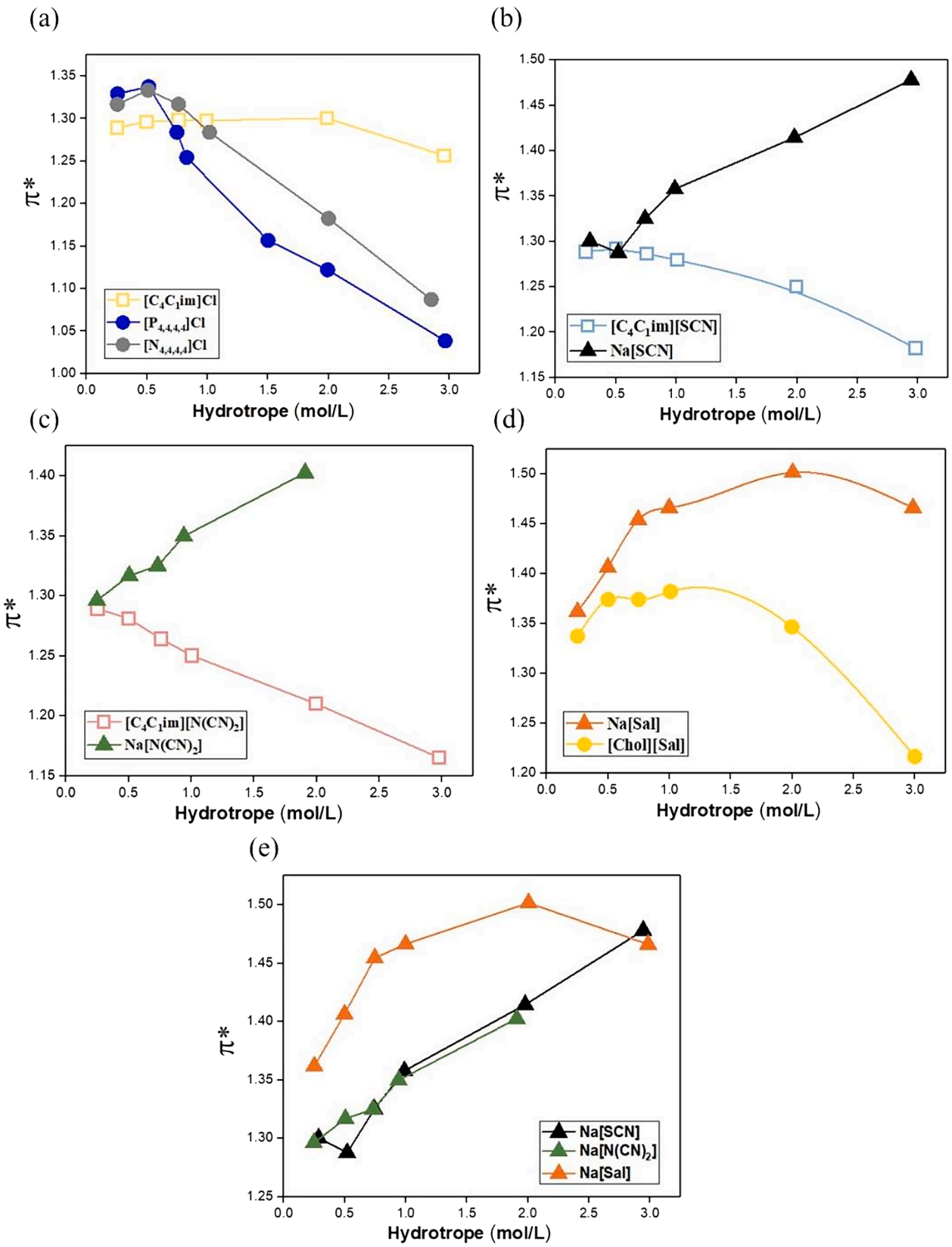

Fig. 9. Dipolarizability/polarizability parameter for hydrotropes aqueous solutions based on: (a) Cl^-; (b) $[SCN]^-$; (c) $[N(CN)_2]^-$; (d) $[Sal]^-$ and (e) Na^+. Solid lines are guides to the eyes. Values for imidazolium-based IL were retrieved from [24].

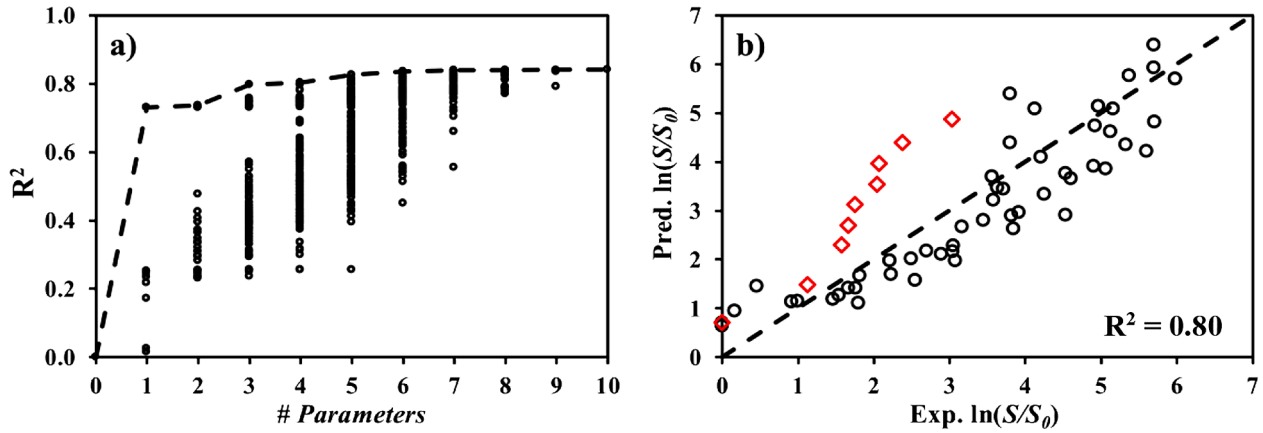

Fig. 10. **a)** Coefficient of determination (R^2) of the regressions between $\ln(S/S_0)$ and all possible combinations of the variables $C_H, \alpha, \beta, \pi^*, \alpha^2, \alpha\beta, \alpha\pi^*, \beta^2, \beta\pi^*, \pi^{*2}$, as a function of the total number of variables used in the regression. The dashed line represents the best R^2 obtained for each different total number of variables. **b)** Performance of the correlation between $\ln(S/S_0)$ and C_H, π^*, and π^{*2}. The dashed line represents equality between predicted and experimental $\ln(S/S_0)$. The data for $[C_4C_1im]Cl$ is highlighted (red diamonds).

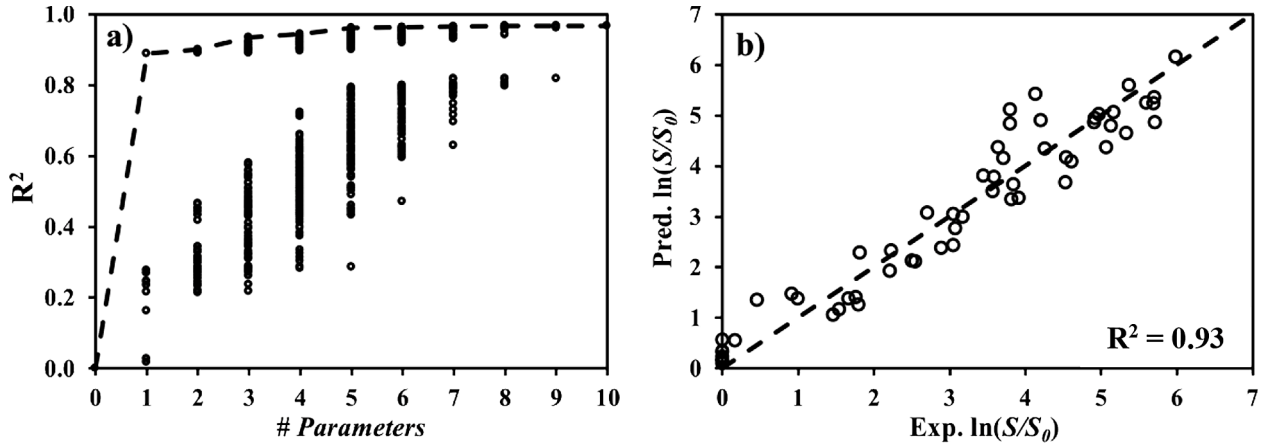

Fig. 11. **a)** Coefficient of determination (R^2) of the linear regressions between $\ln(S/S_0)$ and all possible combinations of the variables $C_H, \alpha, \beta, \pi^*, \alpha^2, \alpha\beta, \alpha\pi^*, \beta^2, \beta\pi^*, \pi^{*2}$, as a function of the total number of variables used in the regression, excluding the solubility data for $[C_4C_1im]Cl$. The dashed line represents the best R^2 obtained for each different total number of variables. **b)** Performance of the correlation between $\ln(S/S_0)$ and C_H, $\alpha\beta$, and π^{*2}, excluding the solubility data for $[C_4C_1im]Cl$. The dashed line represents equality between predicted and experimental $\ln(S/S_0)$.

aqueous solution. Furthermore, salts have greater dipolarizability/polarizability than IL.

Finally, it was shown that empirical correlations based on the hydrotrope concentration and Kamlet-Taft parameters are able to accurately describe the solubility enhancement of artemisinin across different hydrotropic solutions. These results pave the way to the *a priori* design of hydrotropes to solubilize artemisinin, as the correlation can now be used to find the best-performing hydrotrope for this solute, provided that their Kamlet-Taft parameters are experimentally known.

Declaration of Competing Interest

None.

Data Availability

Data will be made available on request.

Acknowledgments

This work was developed within the scope of the projects CICECO-Aveiro Institute of Materials, UIDB/50011/2020 & UIDP/50011/2020, CIMO-Mountain Research Center, UIDB/00690/2020, and Green Health (Norte-01-0145-FEDER-000042) all financed by national funds through the FCT/MEC and when appropriate co-financed by FEDER under the PT2020 and NORTE 2020 Partnership Agreement. Isabela Sales and Silvana Mattedi thanks the finantial support from CAPES and CNPq/Brazil (CAPES: Proc. 88881.189075/2018-01 and 88887.494428/2020-00. CNPq: Grant 303089/2019-9 and Proc.438036/2018-2).

Supplementary materials

Supplementary material associated with this article can be found, in the online version, at doi:10.1016/j.fluid.2022.113556.

References

[1] C.A. Lipinski, F. Lombardo, B.W. Dominy, P.J. Feeney, Experimental and computational approaches to estimate solubility and permeability in drug discovery and development settings, Adv. Drug Deliv. Rev. 64 (2012) 4–17, https://doi.org/10.1016/j.addr.2012.09.019.

[2] R.K. Haynes, B. Fugmann, J. Stetter, K. Rieckmann, H.D. Heilmann, H.W. Chan, M. K. Cheung, W.L. Lam, H.N. Wong, S.L. Croft, L. Vivas, L. Rattray, L. Stewart, W. Peters, B.L. Robinson, M.D. Edstein, B. Kotecka, D.E. Kyle, B. Beckermann, M. Gerisch, M. Radtke, G. Schmuck, W. Steinke, U. Wollborn, K. Schmeer, A. Römer, Artemisone - A highly active antimalarial drug of the artemisinin class,

Angew. Chemie - Int. Ed. 45 (2006) 2082–2088, https://doi.org/10.1002/anie.200503071.
[3] K.L. Chan, K.H. Yuen, H. Takayanagi, S. Janadasa, K.K. Peh, Polymorphism of artemisinin from Artemisia annua, Phytochemistry 46 (1997) 1209–1214, https://doi.org/10.1016/S0031-9422(97)80013-1.
[4] S. Laboukhi-Khorsi, K. Daoud, S. Chemat, Efficient Solvent Selection Approach for High Solubility of Active Phytochemicals: Application for the Extraction of an Antimalarial Compound from Medicinal Plants, ACS Sustain. Chem. Eng. 5 (2017) 4332–4339, https://doi.org/10.1021/acssuschemeng.7b00384.
[5] K. Letchmanan, S.C. Shen, W.K. Ng, R.B.H. Tan, Application of transglycosylated stevia and hesperidin as drug carriers to enhance biopharmaceutical properties of poorly-soluble artemisinin, Colloids Surfaces B Biointerfaces 161 (2018) 83–93, https://doi.org/10.1016/j.colsurfb.2017.10.020.
[6] M. Usuda, T. Endo, H. Nagase, K. Tomono, H. Ueda, Interaction of antimalarial agent artemisinin with cyclodextrins, Drug Dev. Ind. Pharm. 26 (2000) 613–619, https://doi.org/10.1081/DDC-100101276.
[7] Y. Shahzad, S.N.H. Shah, M.T. Ansari, R. Riaz, A. Safdar, T. Hussain, M. Malik, Effects of drug-polymer dispersions on solubility and in vitro diffusion of artemisinin across a polydimethylsiloxane membrane, Chinese Sci. Bull. 57 (2012) 1685–1692, https://doi.org/10.1007/s11434-012-5094-2.
[8] N.G. Sahoo, A. Abbas, C.M. Li, K. Yuen, Solubility enhancement of a poorly water-soluble anti-malarial drug: experimental design and use of a modified multifluid nozzle pilot spray drier, online. 98 (2009) 281–294. https://doi.org/10.1002/jps.
[9] N.G. Sahoo, M. Kakran, L. Li, Z. Judeh, R.H. Müller, Dissolution enhancement of a poorly water-soluble antimalarial drug by means of a modified multi-fluid nozzle pilot spray drier, Mater. Sci. Eng. C. 31 (2011) 391–399, https://doi.org/10.1016/j.msec.2010.10.018.
[10] A.F.M. Cláudio, M.C. Neves, K. Shimizu, J.N. Canongia Lopes, M.G. Freire, J.A. P. Coutinho, The magic of aqueous solutions of ionic liquids: Ionic liquids as a powerful class of catanionic hydrotropes, Green Chem 17 (2015) 3948–3963, https://doi.org/10.1039/c5gc00712g.
[11] S. Shimizu, N. Matubayasi, The origin of cooperative solubilisation by hydrotropes, Phys. Chem. Chem. Phys. 18 (2016) 25621–25628, https://doi.org/10.1039/c6cp04823d.
[12] T. Yin, Y. Chen, W. Shen, Aggregation of an ionic-liquid type hydrotrope 1-Butyl-3-methylimidazolium p-toluenesulfonate in aqueous solution, Colloids Surfaces A Physicochem. Eng. Asp. 564 (2019) 95–100, https://doi.org/10.1016/j.colsurfa.2018.12.032.
[13] B.P. Soares, D.O. Abranches, T.E. Sintra, A. Leal-Duaso, J.I. García, E. Pires, S. Shimizu, S.P. Pinho, J.A.P. Coutinho, Glycerol ethers as hydrotropes and their use to enhance the solubility of phenolic acids in water, ACS Sustain. Chem. Eng. 8 (2020) 5742–5749, https://doi.org/10.1021/acssuschemeng.0c01032.
[14] J. Eastoe, M.H. Hatzopoulos, P.J. Dowding, Action of hydrotropes and alkyl-hydrotropes, Soft Matter 7 (2011) 5917–5925, https://doi.org/10.1039/c1sm05138e.
[15] W. Kunz, K. Holmberg, T. Zemb, Hydrotropes, Curr. Opin. Colloid Interface Sci. 22 (2016) 99–107, https://doi.org/10.1016/j.cocis.2016.03.005.
[16] D.O. Abranches, J. Benfica, B.P. Soares, A. Leal-Duaso, T.E. Sintra, E. Pires, S. P. Pinho, S. Shimizu, J.A.P. Coutinho, Unveiling the mechanism of hydrotropy: Evidence for water-mediated aggregation of hydrotropes around the solute, Chem. Commun. 56 (2020) 7143–7146, https://doi.org/10.1039/d0cc03217d.
[17] M. Hopkins Hatzopoulos, J. Eastoe, P.J. Dowding, S.E. Rogers, R. Heenan, R. Dyer, Are hydrotropes distinct from surfactants? Langmuir 27 (2011) 12346–12353, https://doi.org/10.1021/la2025846.
[18] J.J. Booth, M. Omar, S. Abbott, S. Shimizu, Hydrotrope accumulation around the drug: The driving force for solubilization and minimum hydrotrope concentration for nicotinamide and urea, Phys. Chem. Chem. Phys. 17 (2015) 8028–8037, https://doi.org/10.1039/c4cp05414h.
[19] R.D. Rogers, K.R. Seddon, Ionic liquids - solvents of the future? Science 302 (80) (2003) 792–793, https://doi.org/10.1126/science.1090313.
[20] M.G. Neumann, C.C. Schmitt, K.R. Prieto, B.E. Goi, The photophysical determination of the minimum hydrotrope concentration of aromatic hydrotropes, J. Colloid Interface Sci. 315 (2007) 810–813, https://doi.org/10.1016/j.jcis.2007.07.020.
[21] T.E. Sintra, K. Shimizu, S.P.M. Ventura, S. Shimizu, J.N. Canongia Lopes, J.A. P. Coutinho, Enhanced dissolution of ibuprofen using ionic liquids as catanionic hydrotropes, Phys. Chem. Chem. Phys. 20 (2018) 2094–2103, https://doi.org/10.1039/c7cp07569c.
[22] D.O. Abranches, J. Benfica, B.P. Soares, A.M. Ferreira, T.E. Sintra, S. Shimizu, J.A. P. Coutinho, The impact of the counterion in the performance of ionic hydrotropes, Chem. Commun. 57 (2021) 2951–2954, https://doi.org/10.1039/D0CC08092F.
[23] E.L.P. De Faria, A.M. Ferreira, A.F.M. Cláudio, J.A.P. Coutinho, A.J.D. Silvestre, M. G. Freire, Recovery of Syringic Acid from Industrial Food Waste with Aqueous Solutions of Ionic Liquids, ACS Sustain. Chem. Eng. 7 (2019) 14143–14152, https://doi.org/10.1021/acssuschemeng.9b02808.
[24] I. Sales, D.O. Abranches, P. Costa, T.E. Sintra, S.P.M. Ventura, S. Mattedi, J.A. P. Coutinho, M.G. Freire, S.P. Pinho, Enhancing Artemisinin Solubility in Aqueous Solutions: Searching for Hydrotropes based on Ionic Liquids, Fluid Phase Equilib 534 (2021), 112961, https://doi.org/10.1016/j.fluid.2021.112961.
[25] T.E. Sintra, D.O. Abranches, J. Benfica, B.P. Soares, S.P.M. Ventura, J.A. P. Coutinho, Cholinium-based ionic liquids as bioinspired hydrotropes to tackle solubility challenges in drug formulation, Eur. J. Pharm. Biopharm. 164 (2021) 86–92, https://doi.org/10.1016/j.ejpb.2021.04.013.
[26] M.J. Kamlet, Solvent hydrogen-bond acceptor (HBA) basicities, J. Am. Chem. Soc. 98 (1975) 377–383, https://doi.org/10.1021/ja00418a009.
[27] M.J. Kamlet, J.L. Abboud, R.W. Taft, The Solvatochromic comparison method. 6. The π* scale of solvent polarities1, J. Am. Chem. Soc. 99 (1977) 6027–6038, https://doi.org/10.1021/ja00460a031.
[28] M.J. Kamlet, J.L.M. Abboud, M.H. Abraham, R.W. Taft, Linear solvation energy relationships. 23. A comprehensive collection of the solvatochromic parameters, π, α, and β, and some methods for simplifying the generalized solvatochromic equation, J. Org. Chem. 48 (1983) 2877–2887, https://doi.org/10.1021/jo00165a018.
[29] J. Korner, Choline Gallate and its preparation, US 2589707 A, 1952. https://doi.org/10.1145/178951.178972.
[30] T.E. Sintra, A. Luís, S.N. Rocha, A.I.M.C.L. Ferreira, F. Gonçalves, L.M.N.B. F. Santos, B.M. Neves, M.G. Freire, S.P.M. Ventura, J.A.P. Coutinho, Enhancing the antioxidant characteristics of phenolic acids by their conversion into cholinium salts, ACS Sustain. Chem. Eng. 3 (2015) 2558–2565, https://doi.org/10.1021/acssuschemeng.5b00751.
[31] A.R.R. Teles, E.V Capela, R.S. Carmo, J.A.P. Coutinho, A.J.D. Silvestre, M.G. Freire, Solvatochromic parameters of deep eutectic solvents formed by ammonium-based salts and carboxylic acids, Fluid Phase Equilib 448 (2017) 15–21, https://doi.org/10.1016/j.fluid.2017.04.020.
[32] H. Passos, T.B.V. Dinis, E.V Capela, M.V Quental, J. Gomes, J. Resende, P. P. Madeira, M.G. Freire, J.A.P. Coutinho, Mechanisms ruling the partition of solutes in ionic-liquid-based aqueous biphasic systems – the multiple effects of ionic liquids, Phys. Chem. Chem. Phys. 20 (2018) 8411–8422, https://doi.org/10.1039/C8CP00383A.
[33] P.P. Madeira, H. Passos, J. Gomes, J.A.P. Coutinho, M.G. Freire, Alternative probe for the determination of the hydrogen-bond acidity of ionic liquids and their aqueous solutions, Phys. Chem. Chem. Phys. 19 (2017) 11011–11016, https://doi.org/10.1039/c6cp08210f.
[34] A. Klamt, Conductor-like screening model for real solvents: a new approach to the quantitative calculation of solvation phenomena, J. Phys. Chem. 99 (7) (1995) 2224–2235, https://doi.org/10.1021/j100007a062.
[35] A. Klamt, V. Jonas, T. Bürger, J.C.W. Lohrenz, Refinement and parametrization of COSMO-RS, J. Phys. Chem. A 102 (26) (1998) 5074–5085, https://doi.org/10.1021/jp980017s.
[36] F. Eckert, A. Klamt, Fast solvent screening via quantum chemistry: COSMO-RS approach, AIChE journal 48 (2) (2002) 369–385, https://doi.org/10.1002/aic.690480220.
[37] TURBOMOLE V7.4 2019, A development of University of Karlsruhe and Forschungszentrum Karlsruhe GmbH, 1989-2007, TURBOMOLE GmbH (2007) sinceavailable from, http://www.turbomole.com.
[38] BIOVIA COSMOtherm, Release 2021; Dassault Systèmes.
[39] S. Shimizu, N. Matubayasi, Hydrotropy: Monomer-micelle equilibrium and minimum hydrotrope concentration, J. Phys. Chem. B. 118 (2014) 10515–10524, https://doi.org/10.1021/jp505869m.
[40] J.W. Russo, M.M. Hoffmann, Measurements of surface tension and chemical shift on several binary mixtures of water and ionic liquids and their comparison for assessing aggregation, J. Chem. Eng. Data. 56 (2011) 3703–3710, https://doi.org/10.1021/je200659c.
[41] D.O. Abranches, J. Benfica, S. Shimizu, J.A.P. Coutinho, Solubility Enhancement of Hydrophobic Substances in Water/Cyrene Mixtures: A Computational Study, Ind. Eng. Chem. Res. (2020), https://doi.org/10.1021/acs.iecr.0c03155.
[42] A.R. Harifi-Mood, A. Habibi-Yangjeh, M.R. Gholami, Solvatochromic parameters for binary mixtures of 1-(1-butyl)-3- methylimidazolium tetrafluoroborate with some protic molecular solvents, J. Phys. Chem. B. 110 (2006) 7073–7078, https://doi.org/10.1021/jp0602373.
[43] M.A. Ab Rani, A. Brant, L. Crowhurst, A. Dolan, M. Lui, N.H. Hassan, J.P. Hallett, P. A. Hunt, H. Niedermeyer, J.M. Perez-Arlandis, M. Schrems, T. Welton, R. Wilding, Understanding the polarity of ionic liquids, Phys. Chem. Chem. Phys. 13 (2011) 16831–16840, https://doi.org/10.1039/c1cp21262a.
[44] A.F.M. Cláudio, L. Swift, J.P. Hallett, T. Welton, J.A.P. Coutinho, M.G. Freire, Extended scale for the hydrogen-bond basicity of ionic liquids, Phys. Chem. Chem. Phys. 16 (2014) 6593–6601, https://doi.org/10.1039/c3cp55285c.
[45] P.G. Jessop, D.A. Jessop, D. Fu, L. Phan, Solvatochromic parameters for solvents of interest in green chemistry, Green Chem 14 (2012) 1245–1259, https://doi.org/10.1039/c2gc16670d.
[46] K.A. Kurnia, F. Lima, A.F.M. Cláudio, J.A.P. Coutinho, M.G. Freire, Hydrogen-bond acidity of ionic liquids: an extended scale, Phys. Chem. Chem. Phys. 17 (2015) 18980–18990, https://doi.org/10.1039/c5cp03094c.